Quantitative evaluation measures for assessment of motion registration efficacy in dynamic contrast imaging

Dattesh D Shanbhag[1], Venkata V Chebrolu[1], Sandeep N Gupta[2], Patrice Hervo[3], and Rakesh Mullick[4]

[1]Medical Image Analysis Laboratory, GE Global Research, Bangalore, Karnataka, India, [2]Clinical Systems and Signal Processing, GE Global Research, Niskayuna, NY, United States, [3]GE Healthcare, Buc, France, [4]Diagnostics and Biomedical Technologies, GE Global Research, Bangalore, Karnataka, India

Audience: Scientists and clinicians performing motion correction with dynamic contrast MRI data

Introduction: Dynamic MRI imaging with contrast (4D) is widely used for understanding the functional aspects of disease (e.g. tumor permeability, stroke, myocardial infarction). The extended duration of 4D scan (> 2mins) makes 4D data vulnerable to patient motion. Retrospective motion correction (MC) is therefore employed to correct 4D data and enable accurate quantification; by ensuring that voxels in a given region-of-interest (ROI) are minimally influenced by outside voxels [1]. The evaluation of efficacy of MC is typically performed: (a).visually, (b).Comparing time-series data in a ROI and assessing the degree of dispersion of time-series data (**Fig 1**), (c). Observing certain structures or (d). Difference images **[1]**. Use of difference images is not suitable for quantifying improvement in 4D-MRI since contrast related signal change can confound motion related changes. Therefore the evaluation is at best qualitative in nature and makes comparison of MC efficacy schematic difficult across different sites or vendors. In this work, we describe methods for computing quantitative metrics to test the fidelity of MC with 4D data. The results are presented in different anatomies and different types of motion (rigid/non-rigid), before and after the necessary motion correction.

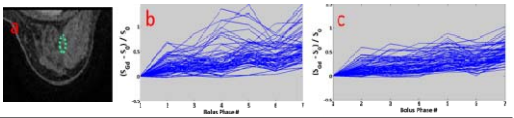

Figure. 1: (a) Visual Evaluation of MC in a ROI; (b) Curves before MC and (c) Curves post MC

Methods and Materials: **Patient Data:** Data for our study was acquired from three different patients, covering head, prostate and breast anatomies with different types of motion: Rigid motion in brain, rigid and non-rigid motion in prostate and non-rigid motion in breast. An appropriate IRB approved each of the studies. **Imaging:** The datasets were obtained on a 1.5T GE Signa Genesis and 3.0T GE Signa HDx clinical scanners (GE Healthcare, Waukesha, WI). The protocol was: ***a. Brain*:** Axial slices, 3D EFGRE sequence with 8-channel brain coil, TE = 1.15ms, TR = 4.9 ms, FA = 10°, slice thickness (TH) = 7mm, matrix size = 512 x 512, FOV = 240x 240 mm^2, 24 bolus volumes, ~7s / volume. ***b. Prostate*:** Axial slices, 3D FSPGR with EIS TORSO coil, TE = 1.3 ms, TR = 3.8 ms, FA = 15°, TH = 6 mm, matrix size = 256 x 256 , FOV = 260 x 260 mm^2, 80 bolus volumes (~4.5 s/ volume), in 6 mins, ***c. Breast:*** Axial slices, 3D VIBRANT with 8-channel HDBreast coil, TE = 2.5 ms, TR = 5.3 ms, FA = 10°, TH = 2 mm, matrix size = 512x512 , 85 slices, FOV = 340 x 340 mm^2, 7 bolus volumes (~76 s/ volume). **Time-series derived metrics:** ***a. Local correlation metric (LCM):*** The 3D time-series signal data (S_t) is first normalized as: $S_{t,norm} = (S_t - S_0)/ S_0$, where S0 is the first time-point signal. The peak time point (t_p) is computed. To avoid noise voxels from corrupting the metric, only those voxels with $max(S_{t,norm}) > 0$ and $min(S_{t,norm} \quad (t > t_p)) > -2.5\%$ are considered in the computation. A given voxel which fails the criteria is assigned a metric value of zero. For a valid voxel, we accumulate only the valid signal time-series curves from a 3x3x3 neighborhood around the voxel. Next a correlation metric is computed among all the accumulated curves. The mean of correlation coefficients is provided as the ***local correlation metric***. Higher the value of LCM better is the alignment of the time-points in a given ROI. ***b. Local dispersion metric (LDM):*** As observed from Fig. 1, both motion and contrast flow cause change in signal data, so a simple time-series distance metric is in-sufficient for demonstrating motion only related changes. However, we observe from Fig. 1 that at each time–point, the variance in data is reduced post motion correction. This forms the basis of the local dispersion metric. First we stack the valid curves in a given 3D neighborhood along the rows. Next at each time point (t), we determine the variance in the data across neighborhood voxels (σ_t^2) (**Fig. 2**). ***Local dispersion*** is then calculated as: $\sqrt{\frac{1}{Nt}\sum_{t=1}^{Nt}\sigma_t^2}$. It should be noted that lower the value of LDM, better is the alignment of the time-points in a given ROI. Entire analysis was performed using the functionality available in MATLAB and ImageJ [**2**]. **Motion Registration:** For each of the data sets, rigid and non-rigid motion correction was implemented using the registration functionality available in ITK framework as follows: ***1. Brain***: Affine transformation with mutual information (MI) metric; ***2. Prostate:*** Combination of affine (MI metric) and level-set optic flow non-rigid correction (sum-of-squares error metric) [**3**] and ***3. Breast:*** Rigid (MI metric) and 3rd order B-Splines based non-rigid correction (MI metric) [**4**]. **Results:**As seen in **Fig.3 (a)**, there is significant motion in prostate DCE-MRI data, which is suitably corrected by the MC algorithm (Fig 3b). For a given ROI in prostate region, we notice that post registration, the curves align well to each other; compared to before registration (Fig 3g). The improvement derived from MC is captured reliably in the LCM and LDM metric (Fig 3c-f). Notice that LCM metric is very homogenous in the region of femoral artery and tissue surrounding prostate gland, compared to original motion corrupted data. As expected, the better alignment of data results in lower LCM values through-out the prostate FOV, post MC (**Fig 3d**). Similar results are demonstrated for brain as well as breast tissue in Figures 4 and 5 respectively. The improvement post MC can be quantified as shown in Figure 4b and c through histograms and statistics in a ROI. **Discussion:** LCM primarily reflects temporal continuity in a given ROI, while LDM captures the spatial continuity in a given ROI. The LCM and LDM maps are thus complimentary and should be used in synchrony for best judgment of motion correction. The LCM and LDM maps can be used as standardized mechanism for reporting improvement in dynamic data after MC (See fig 5c) and allow easy comparison of performance of different algorithms or multi-site MC data. In the current work, we have used the signal intensity data for computation of LCM and LDM metrics. Since the signal data can be corrupted by signal inhomogeneity related artifacts, use of normalized data (e.g. using the baseline signal or concentration mapping) will result in better reliable estimation of LCM metric. The LCM and LDM map fidelity can be further improved by tissue classification and restricting neighborhood to be within a particular tissue type (such as grey matter/white matter in brain). Next, we intend to determine the sensitivity of the method to different degrees and types of motion encountered in specific anatomy.

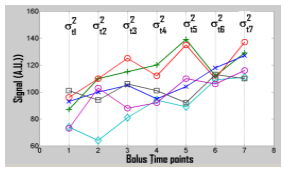

Figure 2: Time-series data arranged for LDM calculation

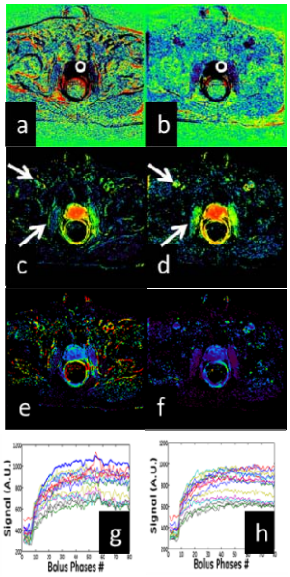

Figure 3: (a) Difference image (t = 0 / 225s) before and (b) after MC. (d).LCM metric following MC shows improvement around prostate and femoral arteries (arrows). (e). LDM indicates spikes before MC and (f). Are subdued following MC. Curves for white ROI (a and b) are shown in g and h

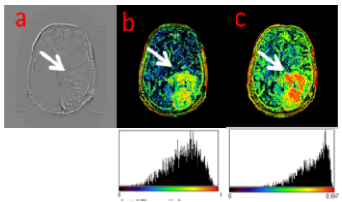

Figure 4: (a). Difference image before and after MC demonstrates change. (b, c). LCM shows marked improvement in region of tumor after MC and is reflected quantitatively in histograms of tumor ROI.

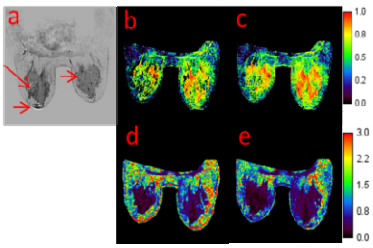

Figure 5: (a) Difference image before and after MC demonstrates change; especially at regions marked by arrows. LCM (b , c) and LDM (d ,e) metric shows marked improvement in these regions after MC

Conclusion: Local correlation and dispersion based measures have been introduced to reliably reflect the improvement in dynamic 4D MRI data tissue alignment post motion correction. These measures can be used as part of motion correction workflow and provide means for quantifying the efficacy of motion correction schemes in dynamic data across different anatomies and clinical sites.

References:

[1]. Kim M., Med. Phys. 39 (1), p.353 . **[2].** Schneider, C.A., Nature Methods 9, 671-675, 2012. **[3].** Vemuri BC, Med. Img. Analy. Vol. 7. p. 1-20. 2003. **[4].** Klein s., IEEE Trans. Med.Img, 29(1):196-205, 2010